Molent Aerostructures
Consulting Pty/Ltd

Bringing you Consultancy, Training, Coaching and novel outcome focused innovative aircraft structural integrity (ASI) solutions and advice

My Doc ID: MAC 1 May22

Attention: Dr M. Fox NTSB

Piper PA-28R-201 Spar Cracking: Preliminary Assessment of Effective Size of Nucleating Discontinuities for aluminium alloy 2024.

RESEARCH TASK DESCRIPTION:

1. OBJECTIVES

To assess the assumption in [1] of a typical nucleating discontinuity depth of 0.01mm deep. The 0.01mm used for aluminium alloy (AA) 2024-T3 in [1] was intended to provide a conservative (in this sense - fast) fatigue crack curve. The author is unaware of specific research studies aimed at assessing typical or mean initiating discontinuity size for AA2024 that are statistically significant. Thus [1] recommended: "As the nucleating discontinuity depth is a critical factor in the analyses, and a typical common depth was used, further investigation of typical discontinuity sizes in AA2024 is warranted and prudent." This preliminary and limited analyses was achieved as follows:

a. A review and initial discontinuity size analyses of cracking in representative aircraft production AA2024 plates; and
b. A review of literature that provided some details of initial discontinuity sizes that cause fatigue crack nucleation and early growth in production quality and finish AA2024-T3 thin sheet (from 0.5 mm to 1.5 mm thick), albeit mainly without analyses.

2. BACKGROUND

Reference [1] summarises analyses conducted to estimate the fatigue crack growth (FCG) likely in cracked AA2024-T3 Piper aircraft spar caps. The principal tool used was the Lead Crack Framework [2] as the usage history of the spars considered was unknown, with only total estimated flight hours and maximum crack sizes available. Key to the Lead Crack approach is the estimation of the fatigue-crack-like effectiveness of the nucleating discontinuity that led to the particular fatigue crack. As it was impractical to do this for the cracks considered, a generic value of 0.01 mm depth [2] was used as the starting point of the FCG analyses. This was intended to provide a (not-overly) conservative estimate of the FCG histories of the subject spars. The resulting analyses is presented in Figure 1.

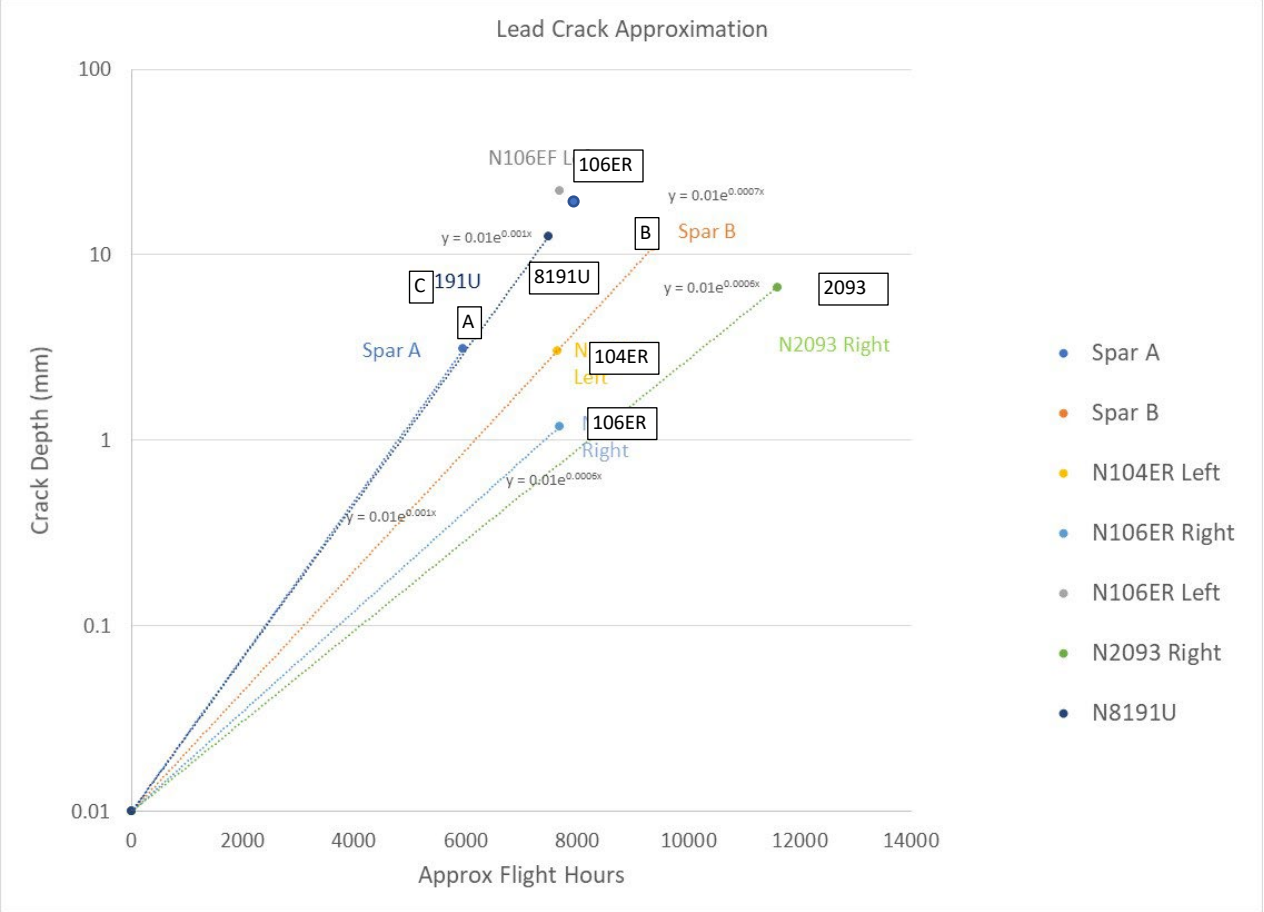

Figure 1: Preliminary estimates of crack growth curves for available cases [1]. It is instructive to note the similar estimated crack growth behaviour of Spar B and Aircraft N104ER left wing, and Spar A, N8191U and N106ER left.

Whilst the author has conducted extensive studies into the effectiveness of initial discontinuities in AA7050 [3-8], he is not aware of similar assessment for AA2024-T3.

2.1 Effectiveness of Initial Discontinuities

Maintaining aircraft airworthiness to ensure the fleet safe operation and maintain its readiness is critically dependent on accurate modelling and reliable predictions of FCG. In this process a knowledge of the representative initial discontinuity sizes, that cause fatigue crack nucleation and early growth in aircraft, is essential.

Whilst many metrics have been proposed to estimate the crack-like effectiveness of initial discontinuities (e.g. depth, area etc) it is now known that despite these metrics not all types of discontinuities (e.g. mechanical damage, inclusions, pits, pores etc) are similarly effective in nucleating FCG [3,5,6] (give the same material, loads, spectrum etc).

Let us now address the definition of the terms equivalent initial flaw size (EIFS) and equivalent pre-crack size (EPS).

Rudd [9], Potter and Yee [11] and Manning and Yang [12] were amongst the first to introduce the concept of an EIFS. Manning et al. [10] then revealed that small crack growth in military aircraft could be expressed in the form:

$$da/dt = Q\, a^b \qquad (1)$$

where Q was both material and spectrum dependent and b was approximately 0.97. In the initial small crack region, it was subsequently recommended [12] that the value of b was taken as 1 so that the crack length could often be expressed in the form:

$$a = a_o e^{\lambda t} \qquad (2)$$

where λ was a constant and a_o was the EIFS. Both [10,12] recommended that the EIFS be determined via quantitative fractography (QF).

Molent et al. [3,5], Molent [6], and Molent, Barter and Wanhill [2] recommended a similar approach and a summary of the application of this approach to cracking in Australian RAAF aircraft is given in [5] where the EPS sizes for AA are shown to range from 0.0077 to 0.129 mm. References [2,7] used the terminology equivalent pre-crack size (EPS), rather than EIFS. This is because although the USAF recommended approach to calculating EIFS [9-12] has not been rescinded, the term EIFS is now commonly used to refer to an "artificial" initial size that when used with AFGROW, FASTRAN, NASGRO, etc would give a reasonable estimate of the total fatigue life.

These two different interpretations of the term EIFS results from statements contained in [9], viz:

a) "If the Equivalent Initial Quality Method is to be used to obtain the initial crack size to be used in economic life predictions, then it may be desirable to obtain good agreement between the analytical prediction and the fractographic test data for crack sizes up to 0.03 inch allowing removal of cracks by reaming the fastener hole to the next nominal hole size." The EPS approach is consistent with this definition of an equivalent initial quality method.

b) “Similarly, if the Equivalent Initial Quality Method is to be used to obtain the initial crack size to be used in establishing inspection intervals or fracture limits, then it may be desirable to obtain good agreement between the analytical prediction and the fractographic test data at failure (ae = ac). The initial crack size (crack size when the load history is first applied), a_i, of the analytical crack growth curve which correlates best with the fractographic test data is defined as the equivalent initial quality.” This definition led to the development of the current EIFS concept.

However, it should be noted that whereas the use of an EIFS can give reasonable values for the total life, the shape of the resultant crack size versus cycles history is often erroneous.

Whilst the original EIFS method relied on the observation of exponential (or log-linear) FGC, there are some differences in the way an EPS is estimated. Importantly the EPS relies on early FCG. This is primarily to avoid potential departures from exponential growth due to factors such as load shedding, changes in component geometry as the crack grows etc (see [5]). In the following analyses judicious choice was made of that early cracking period.

Molent, Barter and Wanhill [2] recommended an EPS of approximately 0.01 mm for 7000 series AA. A comprehensive list of the EPS values associated with 7000 series alloys, evaluated as part of the F/A-18 Hornet program, is given in [3] where the EPS values are shown to range from approximately 0.002 to approximately 0.0774. The EPS value of 0.01 mm recommended in [5] represents the log average of a statistically significant sample size, see [40] and Figure 2. This value was found [5] to hold for both etched and machined specimens and was also shown to correspond to the value associated with numerous full scale fatigue tests (FSFT).

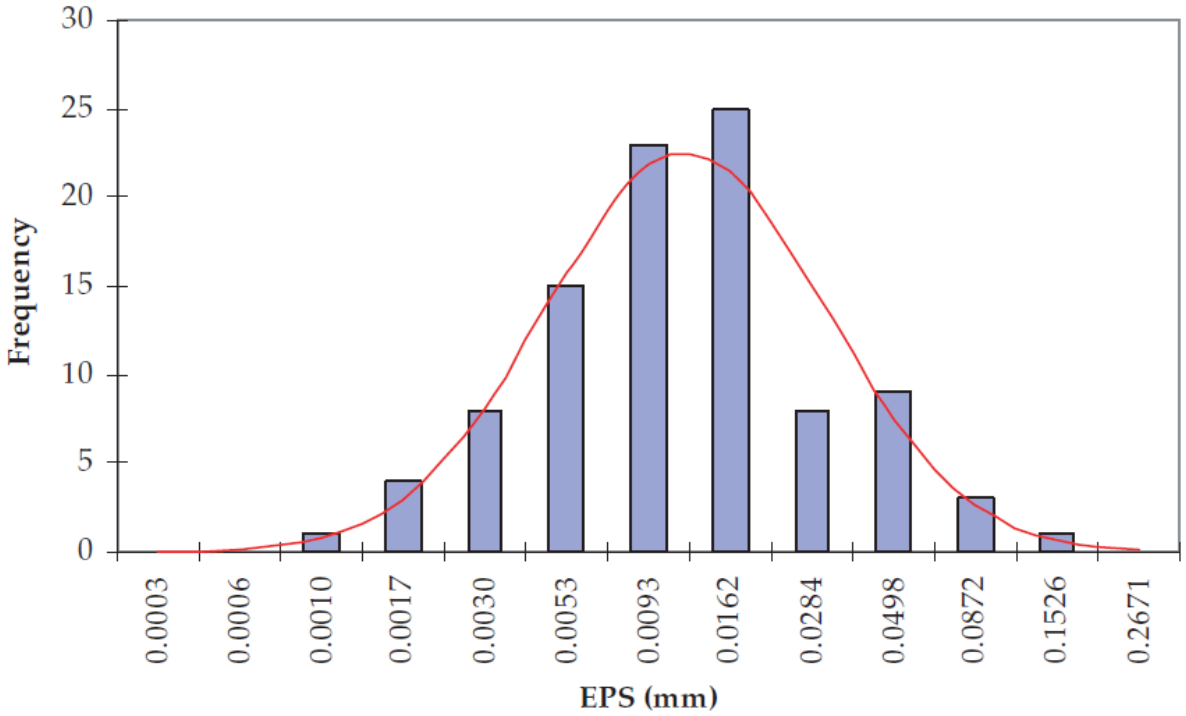

Figure 2: Distribution of EPS values in etched coupons tests, from [5]

Part A: QF data from aircraft representative AA2024.

A review of the literature (as well as unpublished Defence Science and Technology Group (DSTG)) revealed a number of relevant data related either to FSFT or aircraft representative specimens [13-16]. An EPS analyses of these data follow.

a. Pc9 FSFT main spar cracking [13]

Material: AA2024-T3 alloy extrusion

Measurement by QF. Note: most data herein were digitised and is therefore subject to some error.

Post analyses of the Pc9 FSFT conducted at DSTG under service representative loading revealed cracking in several fastener holes about the root of the spar. Each crack was likely to have experienced difference in stress given its location along the spar. The available data is shown in Figure 3 which also contains exponential trend lines which define the EPS. The derived EPS values are given in Table 1.

b. USAF Specimens [14]

Material: AA2024-T851, thickness = 9.525mm, no load transfer (note: the temper is not considered to effect resulting EPS).

Measurement by QF.

These multi-hole, no-transfer specimens were tested under both the F-16 400 hour spectrum and the B-1 Bomber spectrum. Note two different stress levels were tested. The available data is shown in Figure 4 through Figure 6. The derived EPS values are given in Table 1.

c. CT4 Airtrainer full-scale fatigue test main spar [15]

Material: AA2024-T3 extrusion

Measurement: QF (note: available data does not show individual data points (solid line))

Results are from the DSTG FSFT conducted under representative service loads. The available data is shown in Figure 7 which also contains exponential trend lines which define the EPS. The derived EPS values are given in Table 1.

d. Wang Multi-hole coupons [16]

Material: A2024-T3
Measurement: QF

Multi-hole specimens tested under a transport aircraft lower wing spectrum. Two thicknesses considered. The available data is shown in Figure 8 which also contains exponential trend lines which define the EPS. The derived EPS values are given in Table 1.

The data considered represents aircraft production AA2024 tested under various variable amplitude spectra. Different stress levels were considered as well as geometry variations including neat-fit countersink holes.

From this limited analysis a mean EPS for AA2024 of 0.03mm depth was derived. This is larger than the typical EPS value used in [1].

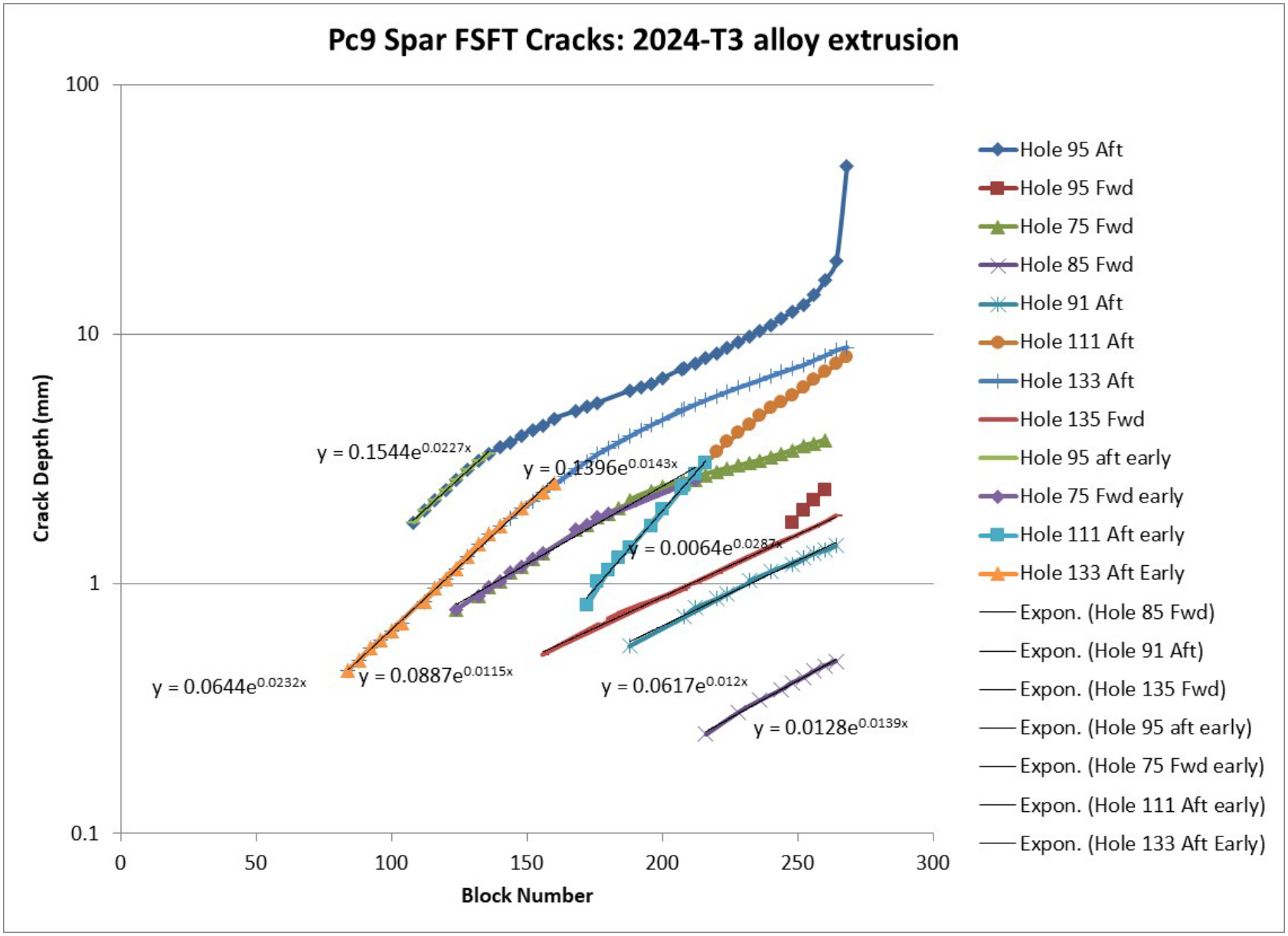

Figure 3: QF derived FCG curves from the DST Pc9 FSFT [13]. Shown are regression fits for the early or total exponential growth period. (Excel: Met Lab Pc9 spar)

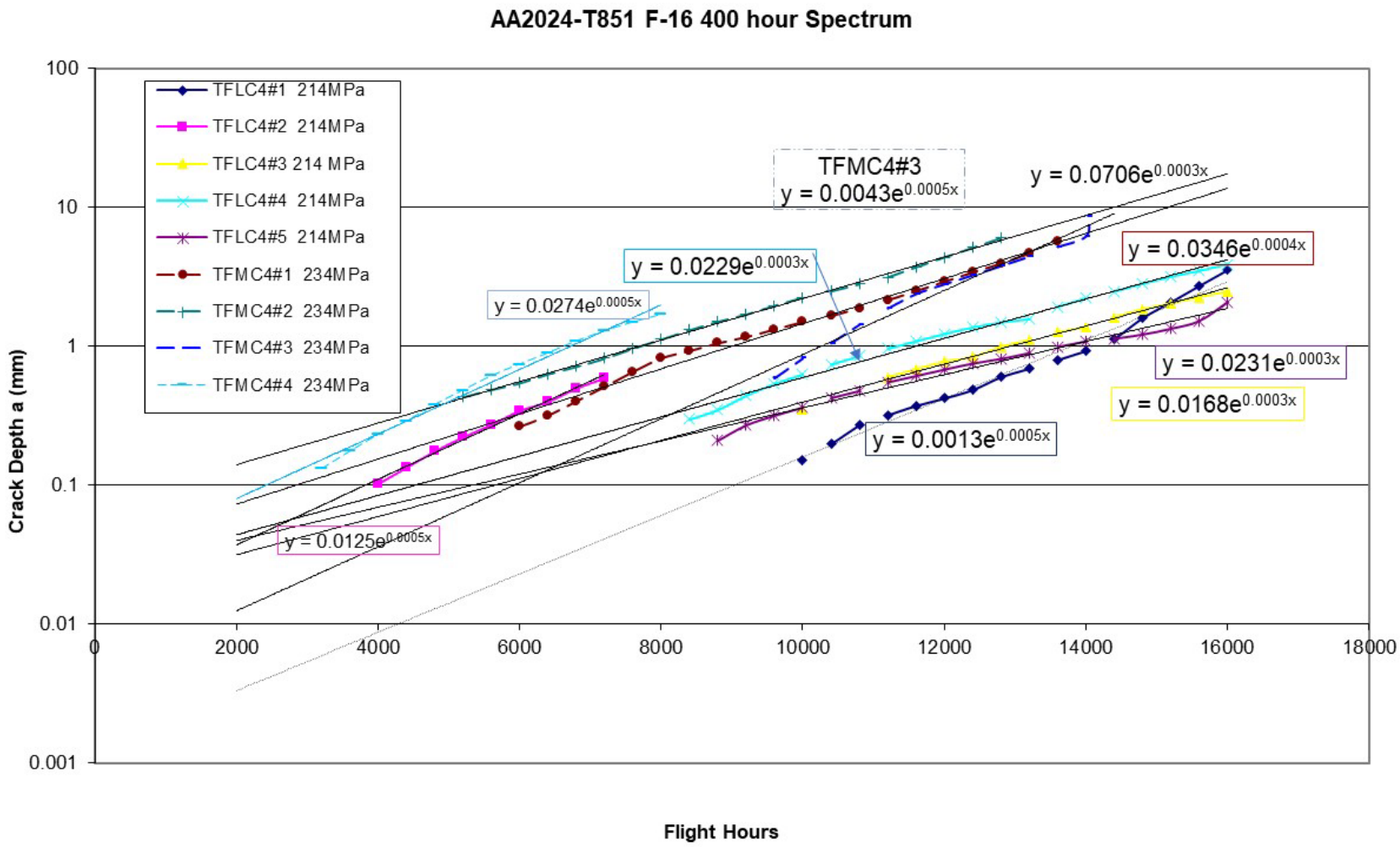

Figure 4: TLFC and TFMC specimens with countersunk holes (NAS1580 fastener), 400 hour F-16 Spectrum [14]. Regression lines shown.

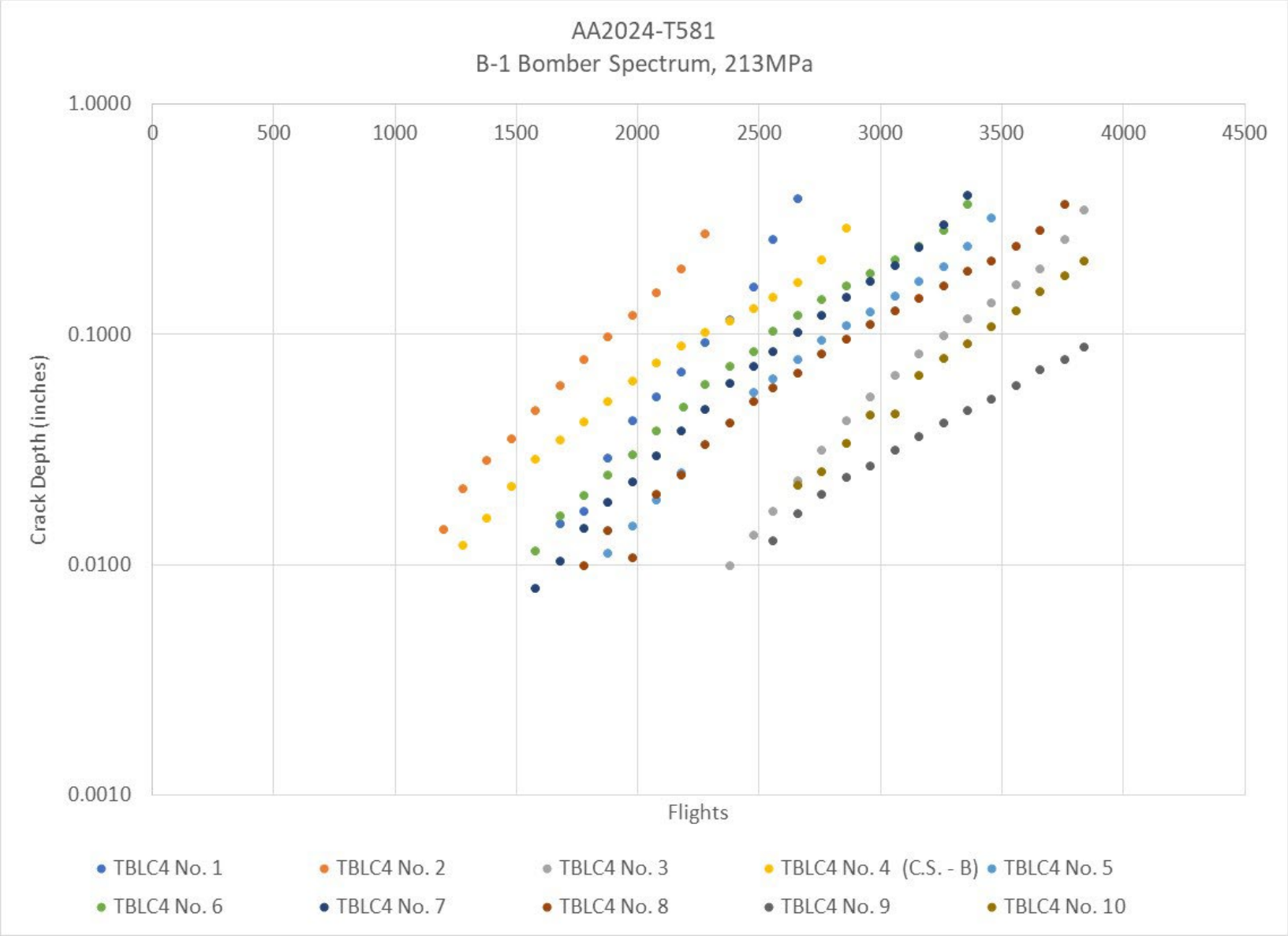

Figure 5: TBLC4, countersunk holes (NAS1580 fastener) B-1B Spectrum [14]. Regression lines not shown for clarity. (Note: Units inches)

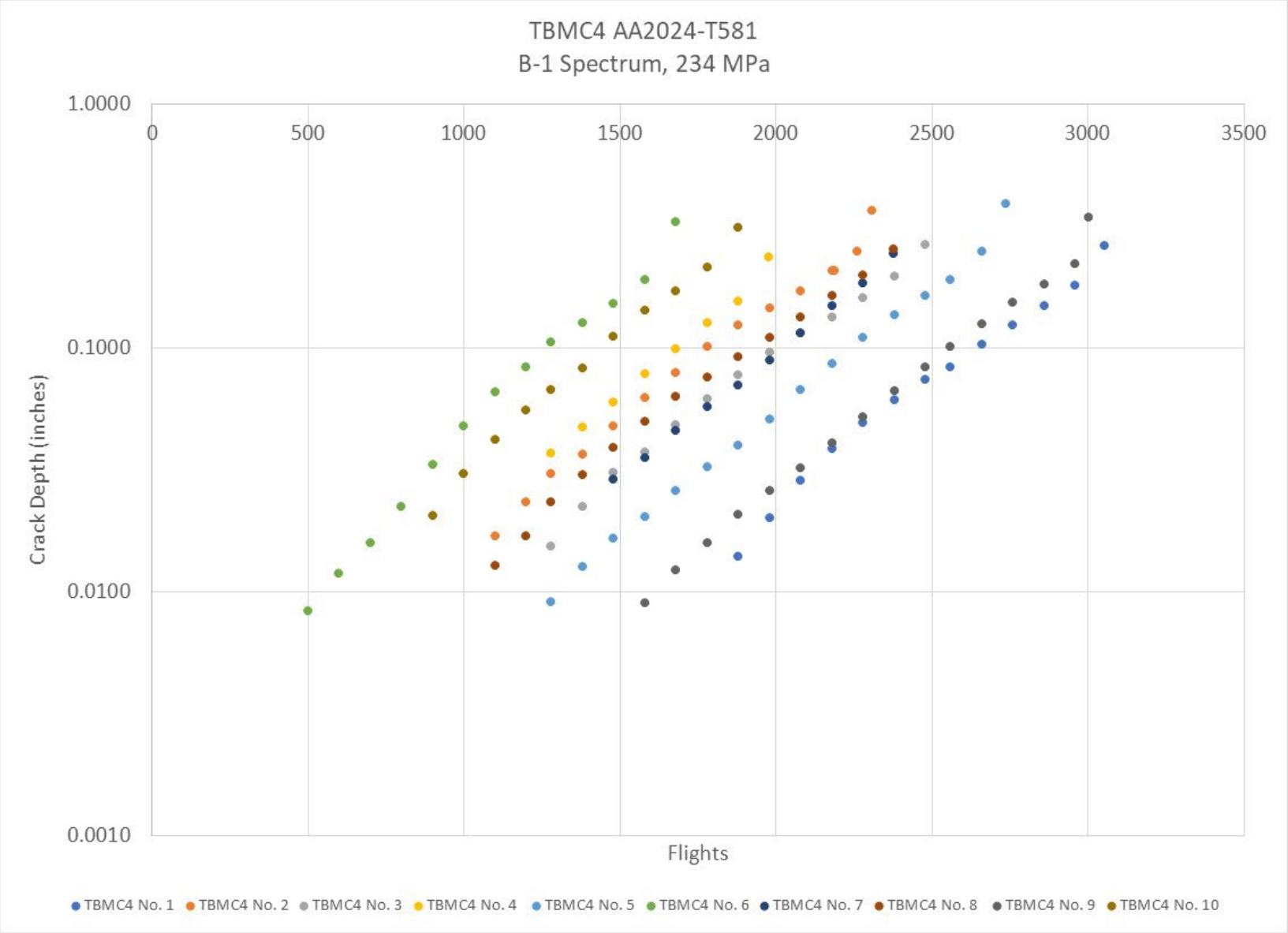

Figure 6: TBMC4, countersunk holes (NAS1580 fastener) B-1B Spectrum [14]. Regression lines not shown for clarity. (Note: Units inches)

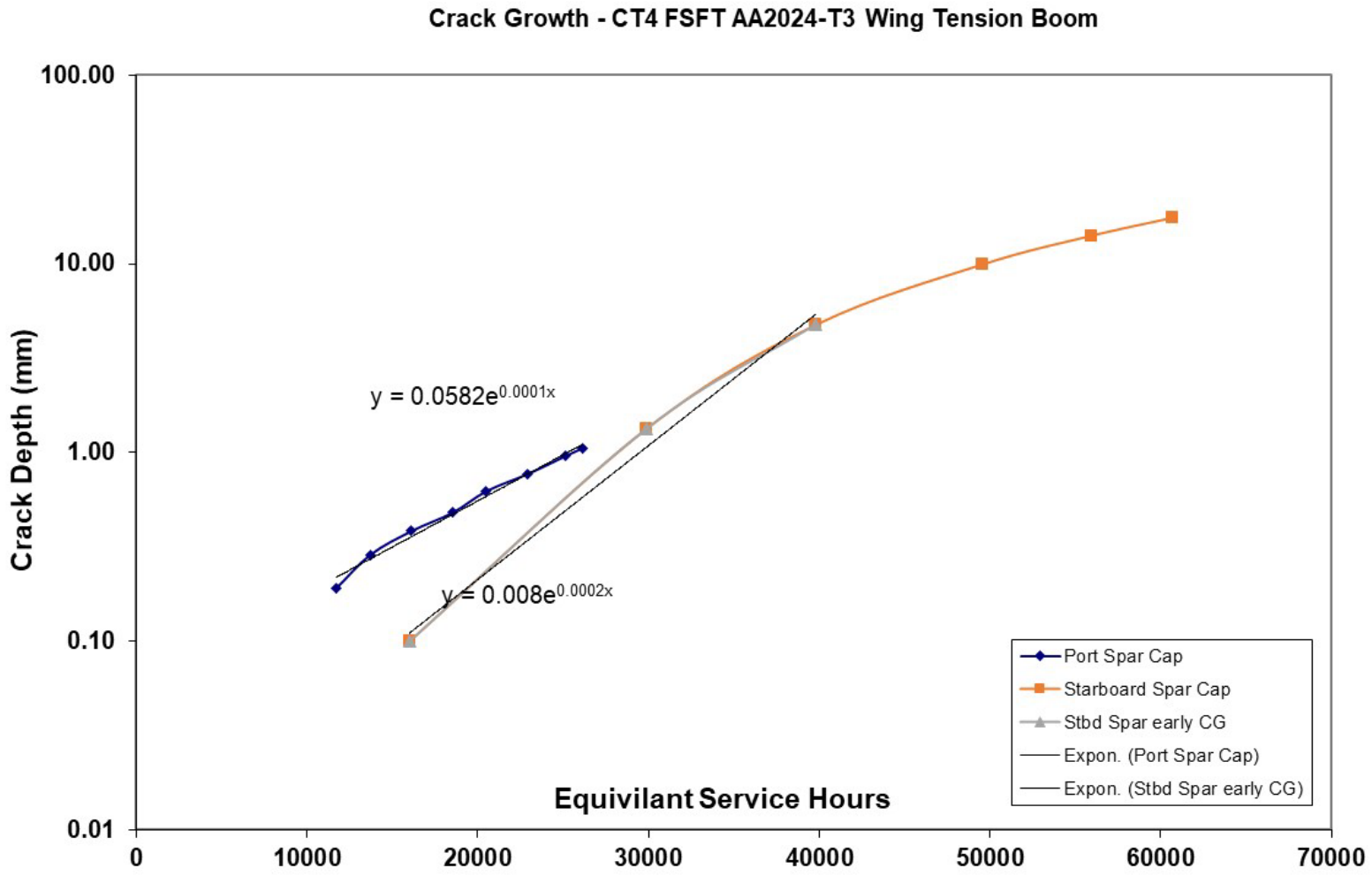

Figure 7: CT4 FSFT main wing spars cracking [15]. Shown are the regression fits. (Excel: CT4 tension boom)

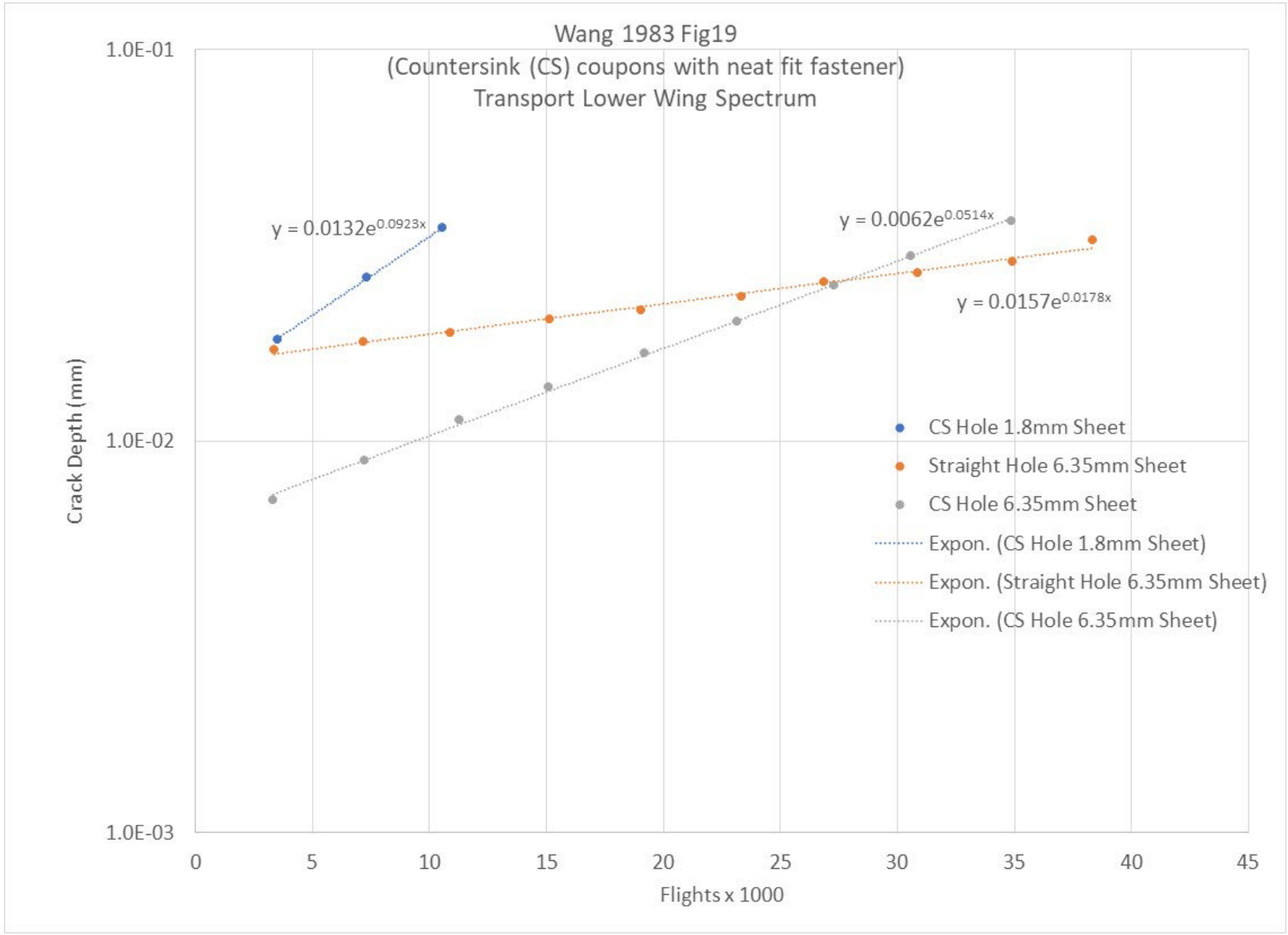

Figure 8: Wang multi-hole coupon results with regression lines shown [16] (from Excel Wang AA2024)

Table 1: Summary of EPS analyses (Excel: AA2024 EPS)

Pc9 FSFT spar cracks [13]	Estimated EPS (mm)	
Hole 95 Aft early growth	0.1544	
Hole 95 Fwd*		
Hole 75 early growth	0.0887	
Hole 85 Fwd early growth	0.0128	
Hole 91 Aft early growth	0.0617	
Hole 111 Aft early growth	0.0064	
Hole 133 Aft early growth	0.0644	
Hole 135 Aft	0.0887	
Average		0.068157

* Too few points

USAF AA2024-T581 Hole Coupons F16 400hr Spectrum [14]		
TFLC4#1 214MPa	0.0013	
TFLC4#2 214 MPa	0.0125	
TFLC4#3 214 MPa	0.0168	
TFLC4#4 214 MPa	0.0229	
TFLC4#5 214 MPa	0.0231	
TFMC4#1 234 MPa	0.0346	
TFMC4#2 234 MPa	0.0706	
TFMC4#3 234 MPa	0.0043	
TFMC4#4 234 MPa	0.027	
Average		0.02368

USAF AA2024-T581 Hole Coupons B-1B Spectrum [14]	
TBLC4#1	0.001632
TBLC4#2	0.018153
TBLC4#3	0.001341
TBLC4#4	0.037231
TBLC4#5	0.007528
TBLC4#6	0.019535
TBLC4#7	0.008924
TBLC4#8	0.013482
TBLC4#9	0.009657
TBLC4#10	0.003637

Average		0.012112
TBMC4#1	0.006038	
TBMC4#2	0.039497	
TBMC4#3	0.027084	
TBMC4#4	0.033452	
TBMC4#5	0.011306	
TBMC4#6	0.053173	
TBMC4#7	0.002718	
TBMC4#8	0.03268	
TBMC4#9	0.005113	
TBMC4#10	0.057005	
Average		0.026807
CT4 FSFT Spars [15]		
Port	0.0582	
Starboard	0.008	
Average		0.0331
Wang Multi-Hole Specimens [16]		
Countersink 1.8mm sheet	0.0132	
Straight Hole 6.35mm sheet	0.0157	
Countersink Hole 6.35mm sheet	0.0062	
Average		0.0117
Total Average		0.02926

Part B: General Literature Review

This section focuses on (physically short) cracking in AA2024-T3 thin sheet material and presents a critical literature review of the reported initial flaw sizes. In the following literature review, the analyses mainly only provided a qualitative assessment of the nucleating discontinuity, not EPS. The review is solely presented in an attempt to bound the range of initial discontinuities.

Issues with data

There are several potential issues with the data reviewed, that may make the estimate of the effective crack like depth of the initial discontinuity difficult if not impossible, including:

1. Many specimens were pre-cracked before fatigue testing. A pre-crack precludes the possibility of defining a measure of the initial discontinuity size.

2. Some FCG data used the average value of cracks either side of a hole etc. (i.e. 2a). Apart for the often-flawed assumption that the cracks either side of the hole are symmetrical, again this technique precludes the measure of the initial discontinuity.
3. Many test specimens were polished or etched before testing, thus potentially eliminating the surface discontinuities.
4. Few of the references conducted qualitative fractography to aid the estimation of the initial discontinuity.
5. The use of the plastic replica technique to measure the crack length history is now known to sometimes effect the crack growth rate.
6. A description of the actual discontinuity type in many cases was not presented.

A Brief Summary of Test Data Associated with Short Crack Growth in Thin 2024-T3 Skins

Table 2 summarises the results from the literature reviewed. The following provides some additional comments.

There have been relatively few studies (or at least found) into the growth of short cracks in thin AA2024-T3 skins [16-41].

The so-called short crack anomaly, whereby short cracks grow faster than long cracks, was first observed by de Lange [17] and Schijve and Jacobs [18]. Schijve and Jacobs [18] reported that cracks in 2 mm thick AA2024-T3 skins can nucleate from defects/inclusions/discontinuities as small as 0.003 mm that were associated with constituent particle sites in the material, see Table 2.

Schijve [24] reported that the nucleating defects/discontinuities/inclusions had sizes between 0.001 to 0.01 mm and once cracks were bigger than approximately 0.13 mm the crack growth rate (da/dN) versus ΔK relationship was similar to that seen for large cracks. Indeed, it is now generally accepted that the short and long crack da/dN versus ΔK relationships often tend to merge a little way into the "Paris" region.

In this context the proceedings of the AGARD conference [27] is noteworthy in that it contains the results of several studies into cracking in AA2024-T3. The paper by Edwards and Newman [27] presented results for 2.3 mm thick AA2024-T3 skins obtained as part of an AGARD round robin study, see Table 2. The single edge notch specimens were chemically polished. This raises the question as to whether the resultant nucleating discontinuity sizes can be assumed to be representative of defects arising in service aircraft.

The AGARD round robin test program used the plastic replica technique to measure the crack length history. Unfortunately, this method is now known to sometimes effect the crack growth rate and as such raises further questions as to the applicability of the data to cracking in service aircraft.

The AA2024-T3 crack growth tests results presented in [27] also had significant scatter and there was little specific information on the size of the nucleating defects. In the one instance where data was presented it was found that the first detectable discontinuity size varied from 0.02 mm to 0.165 mm. In this work there was no attempt to determine the size of the actual initiating defects.

Wanhill and Schra [28] examined crack growth in both 3.8 mm and 2.3 mm thick AA2024-T3 single edge notch specimens under both constant amplitude and the Fokker 100 load spectrum. The surface of the specimens was chemically polished. This again raises the question as to whether the resultant nucleating defect sizes can be assumed to be representative of defects that arise in service aircraft. This study found that crack nucleation could be traced back to discontinuity less than 0.025 mm, see Table 2. It was also found that the aspect ratio a/c, where a was the depth and 2c is the total surface length, of these initial discontinuities varied with the surface length (2c). The test data gave aspect ratio's that varied from approximately 0.4 for values of 2c/t ~ 0.1 to 0.9 as 2c/t approached 0.04. Here t was the specimen thickness. The reason for this is unclear. This finding differed significantly from the results presented in [27] for nominally the same material and specimen geometry.

Swain, Newman, Phillips and Everett [30] reported a significant increase in the crack growth rate associated with short cracks. In this paper, for hot rolled AA2024-T3 single edge notch specimens with a thickness of 2.3 mm, fracture surface examination indicated that crack nucleation occurred primarily at Fe-rich constituent particle sites whose average size varied from 5-15 μm, see Table 2.

Fawaz [31] studied the growth of multi-site damage in 1.6 mm thick AA2024-T3 (clad) lap joints and reported an EIFS of approximately 20 μm. The range of EIFS determined using AFGROW, see Table 2, reported in [31] is given in Table 3. However, it should be noted that in this study there was no attempt to determine the physical size of the actual nucleating defect and that the EIFS sizes reported in [31] may not have reflected the true size of the initial discontinuities.

Piasick and Willard [32] also reported crack growth associated with small pit like initial defects with sizes ranging from approximately 20-30 μm, see Table 2, and with ΔK values well below the long crack threshold in 2 mm thick AA2024-T3 skins. These sizes are consistent with nucleating defect area sizes that ranged between approximately 69 to 649 μm^2, which correspond to diameters of approximately 9.3 and 28.7 μm respectively, in thin (1.6 mm thick) AA2024-T3 skins [33], see Table 2. Piasick and Willard also presented crack growth data associated with various R viz: R = 0.05, 0.7, 0.75 and 0.8, and gave the crack growth rates associated with crack lengths varying from 100 to 1400 μm.

Table 2: Initial flaw/discontinuity/inclusion sizes in the various thin 2024-T3 sheet specimen tests

Reference	Skin thickness (mm)	Range of nucleating flaw sizes	Technique used to measure crack length	Comment on the nature of the tests
de Lange [17]	Not stated	0.07 mm (This was the smallest size that was able to be detected.)	This study used a replica method and as such the results are questionable[#].	The nucleating discontinuity sizes, obtained using back projection, were in the range 0.0028 – 0.029 mm. The specimens were tested under constant amplitude (C/A) loading.
Schijve and Jacobs [18]	2.0 mm	0.06 mm (This represents the smallest size that could be detected.)	Fine scribe lines together with an optical microscope were used to measure crack length.	The back projected EIFSs were in the range 0.0028 – 0.029 mm. Un-modified plate. The specimens were tested under C/A loading with R ~ 0.
Edwards and Newman [27]	2.3 and 3.8 mm	The smallest sizes detected ranged from 0.012 to 0.165 mm.	This study used a plastic replica method and as such the results are questionable.	This AGARD round robin study used SENT specimens with the notch region being chemically polished. The effect of this process on the initial discontinuity sizes is unknown. The notch itself precludes defining a discontinuity size. This makes it difficult to draw any firm conclusions from these tests. Both C/A and variable amplitude tests were performed using FALSTAFF, Inverted FALSTAFF, TWIST, Helix, Fokker 100, etc spectra.

				The FALSTAFF and Inverted FALSTAFF test results were very similar. This suggests that load sequence/load interaction effects may have been small for these small initial discontinuities.
Wanhill and Schra [28]	2.3 and 3.8 mm	Reference [11] states that [12] measured crack sizes down to 0.012 mm. It was not stated if this was the minimum size detected or the actual size of the initiating defect.	This study used a plastic replica method in conjunction with SEM measurements and as such the results are questionable.	Tested with a Fokker 100 wing spectrum. Cracks nucleated as small semi-elliptical surface discontinuity. The nature of which, i.e. pitting or particles, were not discussed.
Cook [29]	1.6 mm	< 0.2 mm (This represents the range of the smallest sizes that were able to be detected.)	This study used a plastic replica method and as such the results are questionable.	Both C/A loading and a range of variable amplitude tests. Specimens were chemically polished prior to testing. The effect of this process on the initial discontinuity sizes is unknown. This makes it difficult to draw any firm conclusions from these tests.
Swain et al. [30]	2.3 mm	Crack nucleation occurred primarily at constituent particle sites whose average size varied from 0.005 – 0.015 mm	This study used a plastic replica method and as such the results are questionable.	SENT specimens tested under C/A loading at R = 0.5, 0, -1 and -2 and the variable amplitude sequences FALSTAFF, Mini-TWIST, and FELIX/28. The specimens were chemically polished prior to testing. The effect

				of this process on the initial discontinuity sizes is unknown. This makes it difficult to draw any firm conclusions from these tests.
Fawaz[@] [31]	1.6 mm	The nucleating discontinuity sizes were not measured.	Quantitative fractography	The EIFS obtained using AFGROW lay in the range 0.007 – 0.056 mm, with a mean of 0.018 mm. C/A tests.
Piasick and Willard [32]	2.0 mm	0.01 – 0.035 mm (This represents the range of the smallest sizes that were able to be detected.)	Both microscope and plastic replica methods used. As such the results are questionable. The resolution of the techniques was stated as 35 µm and 10 µm respectively	C/A tests with the surface of the notch polished using 0.3 pm diamond paste. Specimens were tested in a 1% NaCl solution. Cracks nucleated at the constituent particle pit.
Merati [33]	1.6 mm	0.009 – 0.029* µm	SEM Fractography.	Specimens cut from both new material and clad material taken from retired aircraft. Both the clad and unclad specimens were polished and etched prior to examining the size of the constituent discontinuity. Most of the fatigue cracks in the unclad AA2024-T3 nucleated at constituent particles. In this instance only large iron bearing particles contributed to the crack nucleation process. There was only a weak correlation between the size

				of the nucleating particles and the fatigue life The clad specimens nucleated cracks associated with corrosion pits.
Lee and Sharpe [35]	1.6 mm	< 0.4 mm	Plastic replica method. As such the results are questionable.	Constant amplitude tests at R = 0.5, 0, -1 and -2. All specimens were chemically polished prior to testing. The effect of this cleaning process on the initial discontinuity sizes is unknown. This makes it difficult to draw any firm conclusions from these tests. There was no information on the nature of the nucleating discontinuity.
Wang [16]	6.35 mm	0.007 – 0.030 mm (This represents the range of the smallest sizes that were able to be detected.)	The crack lengths were determined using both optical microscope and fractography.	Open hole specimens and specimens were the hole contained a fastener were subjected to repeated block loading where each block represented 3,843 flights.
Sharpe and Su [39]	2.3 mm	0.020 – 0.2 mm (This represents the range of the smallest sizes that were able to be detected.)	Acetate replicas with some measurements made using an optical microscope. As such the results are questionable.	Constant amplitude tests at R = 0.5, 0, -1. The edges of the specimen, where the cracks nucleated, were chemically etched.

				There was no information on the nature of the nucleating discontinuity.
Walde and Hillberry [40]	1.6 mm	0.014 – 0.070 mm	The initial pit size was measured optically using a JEOL JXA-8600 Superprobe. Some specimens were examined using an ESESM.	Specimens were pre-corroded and then chemically cleaned with HNO_3. The effect of this cleaning process on the initial discontinuity sizes is unknown. This makes it difficult to draw any firm conclusions from these tests. They were then testing under C/A loading at R = 0.02. Crack growth was from the induced corrosion pits.
Chandrasekaran, Taylor, Yoon and Hoeppner [41]	1.52 mm	0.005 – 0.015 mm in the simulated corrosion tests. 0.001 - 0.006 mm in the specimens taken from an in-service panel.	Crack length was monitored using a zoom lens fitted to a Hitachi KP-112 video camera.	All tests were performed under C/A loading with R = 0.1. Prior to testing the base line specimens were corroded in a 5% NaCl solution. This resulted in pit depths ranging from 5 to 15 μm. Cracks nucleated from the initial corrosion pits.
Schmidt, Crocker, Giovanola, Kanazawa and Shockey [42]	0.93 mm	0.001 - 0.060 mm	SEM, optical and replica techniques. As such the results are questionable.	Specimens taken from an in-service B737 aircraft. Specimens were tested in three conditions: with the clad and paint intact (the as received condition), with the paint chemically

				removed (the clad only condition), and with the paint and clad ground off (the bare condition). Testing was conducted in a 0.5 % NaCl aerated solution. Prior to C/A testing the specimens were exposed to this solution for three days. All clad specimen surfaces were polished prior to testing. All specimens had their edges either polished or machined. The effect of polishing on the initial discontinuity sizes is unknown and therefore makes it difficult to draw conclusions from these tests. In the bare material cracks nucleated at constituent particles, whereas in clad material, cracks usually nucleated at or near crystallographic pit colonies. The nucleating discontinuity size was calculated assuming that crack growth was log-linear.

* These values correspond to the diameters of the nucleating defects/discontinuities/inclusions.

[@]These were EIFS values and not true measurements.

It is now known [44] that the replica technique can yield spurious results.

Table 3 Range of EIFS in [31]

Crack Number	Mean EIFS μm
7A6L	24.297
7A6R	30.105
7A7L	18.352
7A7R	10.763
7A8L	6.704
7A12R	21.492
7A13R	11.856
7A14L	56.426
7A14R	22.517
7A15R	15.279
7A16L	22.380
7A16R	6.321
7A17L	7.254
7A17R	33.931
8A10L	45.316
8A10R	37.294
8A19L	10.688
Average	22.41

Lee and Sharpe [35] also studied crack growth in 2.3 mm thick AA2024-T3 SENT specimens. They also found that cracks nucleated mostly at the inclusion particles, see Table 2. This conclusion is similar to that presented by Bowles and Schijve [36] where it was found that, for 3.57 mm thick AA2024-T3 clad bars, 1-10 μm inclusions led to fatigue crack nucleation.

Wang [16] performed flight-simulation tests, with a cargo transport spectrum on 1.8 and 6.35 mm thick AA2024-T3 multi-hole specimens. Many specimens were counter sunk and contained a neat fit fastener. A limited sample of FCG curves were provided. The size of these nucleating discontinuities was estimated both optically and using quantitative fractography. It was noted that smaller size discontinuities could not be determined due to rubbing of the fracture surfaces. As such these sizes represent the smallest sizes that could be determined rather than the actual initial discontinuity sizes, see Table 2. Wang also reported that the average EIFS size was in the order of 20.0 μm, see Figure 9. The modelling of the EIFS was not detailed.

Sharpe and Su [39] tested 2.3 mm thick AA2024-T5 specimens at stress R's of 0.5, 0.0 and -1. The first cracks that could be detected in these tests had sizes that ranged from approximately 35 μm to approximately 200 μm, see Tables 1 and 4. Walde and Hillberry [40] tested pitted 1.6 mm thick AA2024-T3 specimens and found growth associated with pits with depths ranging from approximately 47 μm to approximately 66 μm, see Tables 2 and 5. Chandrasekaran, Taylor, Yoon and Hoeppner [41] studied the growth of cracks from simulated corrosion pits in 1.52 mm thick AA2024-T3 panels and found growth associated with 5-15 μm defects as well as for 1-6 μm pits that were associated with an in-service component. Schmidt, Crocker, Giovanola, Kanazawa and Shockey [42] presented the results of an extensive study into crack growth in 0.93 mm thick AA2024-T3 skins that were cut from a retired Boeing 737 aircraft. The aircraft line number was 176, entered service in 1968 and was retired in February 1992 having experienced 56,228 flight hours. In this instance the nucleating crack/discontinuity ranged from 5 to 60 μm.

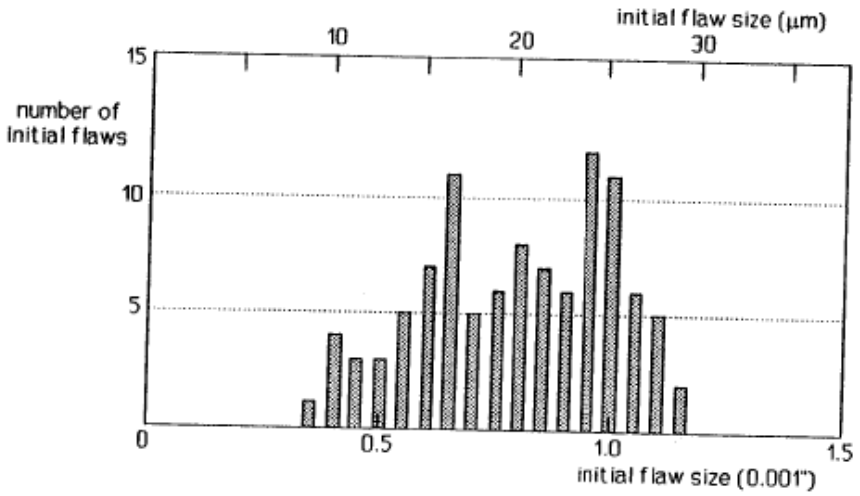

Figure 9: Distribution of EIF's in the tests reported in [16].

Table 4: Size of crack when first observed in 2.3 mm thick AA2024-T5 in [39].

Specimen number	Stress ratio	Size of the first crack found (μm)
B-10	0.5	155
B-11	0.5	70
B-12	0.0	200
B-06	0.0	30
A-126	0.0	20
B-04	-1.0	35
B-02	-1.0	80
B-07	-1.0	50
B-08	-1.0	35
B-09	-1.0	45

Table 5: Summary of random plane pit depth measurements in 1.6 mm thick AA2024-T3, from [40].

Specimen number	Depth μm
1	47.60
2	54.51
3	59.02
4	66.23

Discussion on General Review

These primary findings associated with these studies have been summarised in Table 2 which reveals that many of the studies used replica techniques to determine the crack length histories. Unfortunately, it is now known that such procedures can significantly influence crack growth both under constant amplitude and spectrum loading tests, see [44] page 29. Thus the significance and the applicability of the results associated with these tests to cracking in service aircraft is questionable. In many cases the discontinuity type was not described.

Whilst [27-30] studied crack growth under representative operational load spectra these tests did not use specimens taken from in-service aircraft and as such may not have had representative initiating discontinuities. Furthermore, each of these particular studies used the plastic replica technique to determine the crack length histories and as such, as commented above, the results of these tests are questionable. In this context with the exception of [33], which tested specimens made from a retired C-130 aircraft, [41] which tested some specimens made from the JSTAR (B707) fuselage panel, and [42], which tested specimens made from a retired Boeing B737 aircraft, the other specimen tests had either tested pristine specimens, pre-notched specimens or specimens with induced corrosion pits. As such the associated initial crack lengths may not reflect those naturally occurring defects associated with AA2024-T3 material in-service

Despite the shortcomings inherent in many of these tests, crack growth was, as stated in [24, 33, 41, 42], due to either crack nucleation at constituent particles, mechanical damage or near crystallographic pit colonies. As such these nucleating defects were similar to those reported in [2] for other aerospace quality aluminium alloys. The above brief review suggests that crack growth in thin AA2024-T3 skins can occur from flaws/discontinuities/inclusions as small as 10-30 μm, see Table 2.

Initial Discontinuity Size

Despite the differences in materials, surface finish and specimen thicknesses both the range and the mean value, i.e. an EPS of 0.01 mm, of the EPS's given in [3,5,6] are similar to the range and the mean value (0.018 mm) of the EIF's given by Fawaz [31] for 1.6 mm thick AA2024-T3. These mean values are also similar to the value of 0.008 mm determined by the USAF, in conjunction with General Dynamics, for cracking in AA7475-T7651 [11] as well as to the values for cracking in F4E and A-7 aircraft [9]. Furthermore, the range of the EPS suggested in [2] and the range of the EIFS suggested in [31] for 1.6 mm AA2024-T3 are both similar to the range in the nucleating discontinuities, i.e. 69-647 μm^2, associated with thin (1.6 mm thick) AA2024-T3 skins [33] and the size of the other nucleating discontinuities reported above, see Table 2.

Preliminary Conclusions from General Literature Review

It would appear that:

- Most of the data is associated with tests where either the replica technique was used to determine the crack length histories, which thus casts doubts on the results, or where the specimens were polished or chemically polished prior to testing, which makes the surface finish unrepresentative of service aircraft. As such these results are of limited value.

- There is thus little data associated with the nucleation and growth of natural cracks in 0.05 to 1.5 mm thick AA2024-T3 skins.

- This lack of data means that it is not possible to make meaningful statements about the effect of sheet thickness on the size of the nucleating discontinuities.

- There is minimal data associated with the nucleation and growth of naturally occurring cracks in specimens fabricated from in-service material.

- There is a scarcity of data associated the nucleation and crack growth of naturally occurring cracks under variable amplitude (operational) loading in thin AA2024-T3 skins.

- Despite the limited data and the shortcomings associated with many of the tests the data presented in Table 2 suggest that crack growth in thin AA2024-T3 skins can nucleate from discontinuities/flaws/inclusions as small as 10-30 μm.

- It also appears that, as suggested by Wanhill [43], the fatigue threshold associated with these naturally occurring short cracks in thin AA2024-T3 is very low.

In 1994 Schijve [38] concluded

"The lack of experimental data on crack growth and residual strength, more than 5 years after the Aloha accident, is surprising. There is indeed a great need for systematic experimental investigations on these issues. For the growth of small cracks some kind of marker loads should be used."

The situation does not appear to have changed significantly.

Conclusions

This literature review and analyses attempted to address the recommendation [1] to estimate effective initial discontinuity sizes specifically for AA2024.

The first part considered available quantitative fractography data for tests representative of aircraft production quality AA2024 (including from two FSFTs). From these data a preliminary EPS of approximately 0.03mm deep was derived.

The second part conducted a general literature review in which the size of nucleating discontinuities was addressed. Despite limitations in the available data a lower bound initial discontinuity of approximately 0.01mm was determined. No evidence of spectrum or stress influences were noted.

These results are considered to support the use of a typical EPS of 0.01mm for the spar cracking analyses summarised in [1].

Acknowledgement

Abridged sections of Part B were provided to the author by Prof. Rhys Jones of Monash University (2013).

REFERENCES

1. Molent L. Piper PA-28R-201 Spar Cracking: Summary and Recommendations, MAC 4 Mar22, Molent Aerostructures, Melb., Aust., 18Mar22.
2. Molent L, Barter SA and Wanhill RJH. The Lead Crack Fatigue Lifing Framework, Int Fatigue; 33 (2011) 323–331.
3. Molent L. and Sun Q, The compendium of F/A-18 Hornet crack growth data Version II: Part I, DSTO-TR-2488, November 2010.
4. Molent L., Fatigue crack growth from flaws in combat aircraft, International Journal of Fatigue, 32, (2010), 639–649.
5. Molent L., Sun Q., and Green AJ., Characterisation of equivalent initial flaw sizes in 7050 aluminium alloy, Fatigue Fract Engng Mater Struct 29, (2006), 916–937. 56.
6. Molent L. (Invited Review paper), A review of equivalent pre-crack sizes in aluminium alloy 7050-T7451, Fat Fract Eng Mat Struct 2014;37: 1055-74.

7. Gallagher JP and Molent L. Effect of load spectra and stress magnitude on crack growth behaviour variability from typical manufacturing defects. Advanced Materials Research Vols. 891-892 (2014) pp 100-105.
8. Barter SA, Molent L, Wanhill RJH. Typical fatigue-initiating discontinuities in metallic aircraft structures, J Fatigue 2012 ; 41:11-22.
9. Rudd JL., Application of the equivalent initial quality method, AFFDL-TM-77-58-FBE, July 1977.
10. Manning S.D., Pendley B.J., Garver W.R., Speaker S.M., Henslee SP. Smith VD., Norris JW., Yee BGW, Shinozuka M., and Yang YN.,"Durability Methods Development, Volume I - Phase I Summary," Air Force Flight Dynamics Lab., AFFDL-TR-79-3118, September 1979.
11. Potter J.M., Yee .GW. Use of small crack data to bring about and quantify improvements to aircraft structural integrity, Proceedings AGARD Specialists Meeting on Behaviour of Short Cracks in Airframe Structure, Toronto, Canada, 1982.
12. Manning SD. and Yang YN., USAF durability design handbook: Guidelines for the analysis and design of durable aircraft structures, AFWAL-TR-83-3207, 1984.
13. Interim Report, Quantitative Fractography of PC9 Wing Spar Lower Flange Fracture at Rib 5, by Rohan Byrnes, DST, April2000.
14. Speaker, SM Gordon DE, Kaarlela WT, Meder A, Nay RO, Nordquist FC and Manning SD. Durability method development, volume VIII – Test and fractography data. 1982. Air Force Flight Dynamics Laboratory, Wright-Patterson Air Force Base, AFFDL-79-3118.
15. Parker RG. CT4 Airtrainer full-scale fatigue test, ARL-STRUCT-R-437, DSTO Melbourne 1989.
16. Wang D.Y., A study of small crack growth under transport spectrum loading. AGARD-CP 328, paper 14, 1983
17. de Lange RG., Plastic replica methods applied to the study of fatigue phenomena. Trans. Metallurgical Society, 230, pp 644, 1964.
18. Schijve J. and Jacobs FA., Fatigue crack propagation in notched and unnotched aluminium alloy specimens. NLR TR M-2128, 1964.
19. Pearson S. Initiation of fatigue cracks in commercial aluminium alloys and the subsequent propagation of very short cracks, Engineering Fracture Mechanics, 7, (1975), 235-247.
20. Miller, K. J., The behaviour of short fatigue cracks and their initiation. Part I - A review of two recent books. Fatigue and Fracture of Engineering Materials and Structures, (1987), Vol. 10, No. 1: 75-91.
21. Miller, KJ., The behaviour of short fatigue cracks and their initiation. Part II - A general summary. Fatigue and Fracture of Engineering Materials and Structures. 10, 1, (1987), 75-91.
22. Suresh S, Ritchie RO. Propagation of short cracks. Int Metals Reviews 1984; 29(6): pp 445-476.
23. Schijve J., Fatigue of structures and materials in the 20th century and the state of the art. International Journal of Fatigue, 25, (2003), 679-702.
24. Schijve J., Differences between the growth of small and large fatigue cracks. The relation to threshold K values, Proceedings International Symposium on Fatigue thresholds, Stockholm, Sweden, 1-3 June, 1981. Editors J. Backlund, A. F. Blom and C. J. Beevers, p 881-891, 1982.
25. Jones R. and Molent L., Critical review of the Generalised Frost-Dugdale approach to crack growth in F/A-18 Hornet structural materials, DSTO-Research Report 0350, March 2010.
26. Edwards PR. and Newman JC., Short crack growth behaviour in various aircraft materials, AGARD Report 767, ISBN 92-835-0577-8, August 1990.
27. Edwards PR. and Newman JC., An AGARD supplemental test program on the behaviour of Short cracks under constant amplitude and aircraft spectrum loading, Paper 1, AGARD Report 767, ISBN 92-835-0577-8, pages 1-1 to 1-43, August 1990.
28. Wanhill RJH. and Schra L., Short and long fatigue crack growth in 2024-T3 under Fokker 100 spectrum loading, Paper 8, AGARD Report 767, ISBN 92-835-0577-8, pages 8-1 to 8-26, August 1990.
29. Cook R., The growth of short fatigue cracks in aluminium alloys, DRA technical Report 9263, 1992.
30. Swain MH., Newman JC., Jr., Phillips EP., Everett RA., Fatigue crack initiation and small crack growth in several airframe alloys, NASA Technical Memorandum 102598, January 1990.
31. Fawaz SA., Equivalent initial flaw size testing and analysis of transport aircraft skin splices, Fatigue Fracture Engineering Materials and Structures 26, (2003) 279-290.
32. Piascik RS and Willard SA., The growth of small corrosion fatigue cracks in alloy 2024, Fatigue Fract. Engng Mater. Struct. Vol. 17, No. 11, pp. 1247-1259, 1994.

33. Merati A., A study of nucleation and fatigue behavior of an aerospace aluminum alloy 2024-T3, International Journal of Fatigue, 27, (2005), 33–44.
34. Swain, M. H.; and Newman, J. C., Jr.: On the use of marker loads and replicas for measuring growth rates for small cracks. Presented at AGARD Specialists Meeting, Siena, Italy, April 1984.
35. Lee JJ. and Sharpe WN., Jr, Short fatigue crack behavior in notched 2024-T3 aluminum specimens, NASA-CR 180314, Jan 1984.
36. Bowles CQ. and Schijve J., The role of inclusions in fatigue crack initiation in an aluminium alloy, Int. Journ. of Fracture, 9 (1973) 171-179.
37. Wang D.Y., A study of small crack growth under transport spectrum loading. AGARD-CP 328, paper 14, 1983.
38. Schijve J., Fatigue life until small cracks in aircraft structures durability and damage tolerance, FAA/NASA International Symposium on Advanced Structural Integrity Methods for Airframe Durability and Damage Tolerance, NASA Conference Publication 3274, Editor C.E. Harris, Part 2, pp. 665-681, Hampton, Virginia (1994).
39. Sharpe W.N., Jr and Su X., Closure measurements of naturally initiating small cracks, Engineering Fracture Mechanics Vol. 30, No. 3, pp. 275-294, 1988.
40. van der Walde K., Hillberry BM., Initiation and shape development of corrosion-nucleated fatigue cracking, International Journal of Fatigue 29, (2007) 1269–1281.
41. Chandrasekaran V., Taylor AMH., Yoon Y. and Hoeppner DW., Quantification and correlation of pit parameters to "small" fatigue cracks, Proceedings ICAF '99, International Congress on Aeronautical Fatigue, Seattle, 12-16 July, 1999, Seattle USA, June, Edited by J. L. Rudd and R. M. Bader.
42. Schmidt CG., Crocker JE, Giovanola JH., Kanazawa CH., Shockey DA., Characterization of early stages of corrosion fatigue in aircraft skin, DOT/FAA/AR-951108, February 1996.
43. Wanhill RJH., Characteristic stress intensity factor correlations of fatigue crack growth in high strength alloys: reviews and completion of NLR investigations 1985-1990, NLR-TP-2009-256, September 2009.
44. Newman, J.C., X.R. Wu, S.L. Venneri, and C.G. Li, Small-crack effects in high-strength aluminium alloys, NASA Pub 1309, May 1994.

L. Molent
16 June 2022

Loris Molent AM – Director
ABN 655464494
Phone: +61 413 474 318
E: clanmolent@bigpond.com